Electronic Supplementary Information

Structure dependent luminescence, peroxidase mimetic and hydrogen peroxide sensing of Samarium Doped Cerium phosphate nanorods

G. Vinothkumar[a], Arun. I.L[a], P. Arunkumar[ab], Waseem Ahmed[a], Sangbong Ryu[b], Suk Won Cha[bc], K. Suresh Babu[a]*

[a] Centre for Nanoscience and Technology, Madanjeet School of Green Energy Technology, Pondicherry University, R V Nagar, Kalapet, Puducherry – 605 014, India.

[b] School of Mechanical and Aerospace Engineering, Seoul National University, San 56-1, Daehak dong, Gwanak-gu, Seoul 08826, Republic of Korea.

[c]Institute of Advanced Machines and Design, Seoul National University, Gwanak-Gu Gwanak-Ro1, Seoul 151-742, Republic of Korea

*Corresponding author e-mail: *sureshbabu.nst@pondiuni.edu.in*

Phone: +91-413-2654976

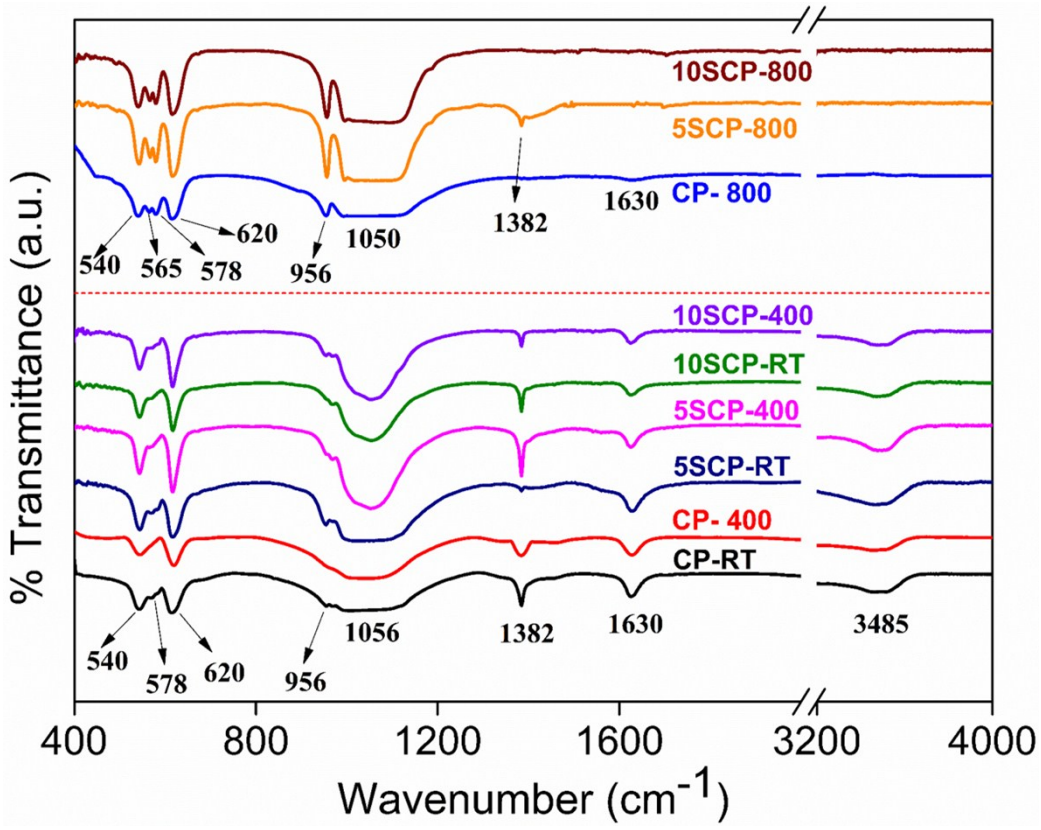

Figure S1. FTIR spectra of cerium phosphate nanorods in the as-prepared and annealed conditions (400 °C and 800 °C)

Fourier Transformed Infrared (FT-IR) Spectra

Figure S1. shows the FTIR spectra of hexagonal and monoclinic $CePO_4$ nanorods measured in the frequency range of 400 – 4000 cm^{-1}. Free PO_4^{3-} group exhibit non-degenerate symmetric stretching vibrations (ν_1) corresponding to P-O bond, triply degenerate antisymmetric P-O bond vibrations (ν_2) in the higher energy region, while doubly degenerate bending vibrations (ν_3) of O-P-O bond and triply degenerate bending vibrations (ν_4) of O-P-O can be observed at lower frequency side. In the present case, a broad band was observed in the range 3300 cm -3500 cm^{-1} which can be attributed to the O-H stretching vibrations and a weak band at 1630 cm^{-1} emerge from the H-O-H bending modes of vibration due to adsorbed water molecules in all the samples. The absence of vibrational bands corresponding to water moieties

in monoclinic samples (annealed at 800° C) is consistent with the TG-DTA analysis. In particular, no significant change in the vibrational characteristics were observed for the as-prepared and 400 °C samples, which indicate no structural modification occurred in the hexagonal phase. The bands at 956 and 1050 cm^{-1} correspond to the asymmetric stretching vibration of P-O in the PO_4^{3-} group[1].

Particularly, the peak at 956 cm^{-1} is well separated and relatively stronger in monoclinic structure compared to all hexagonal $CePO_4$. Two prominent peaks at 540 cm^{-1} and 620 cm^{-1} in the lower frequency range arise from the asymmetric bending vibrations of O-P-O bond in the hexagonal structure. However, additional bands at 565 cm^{-1} and 578 cm^{-1} were clearly observed in the monoclinic structure due to the change in the 8-fold coordination (hexagonal) to 9-fold coordination of Ce atoms in the lattice. Various PO_4^{3-} vibrational bands in both structure and presence of additional bands in the monoclinic structure are in good agreement with the Raman spectroscopy. Moreover, the absence of meta- and pyrophosphate peaks in the region between 730 cm^{-1} to 750 cm^{-1} in the spectrum indicates the phase purity of the as-prepared and annealed samples[2].

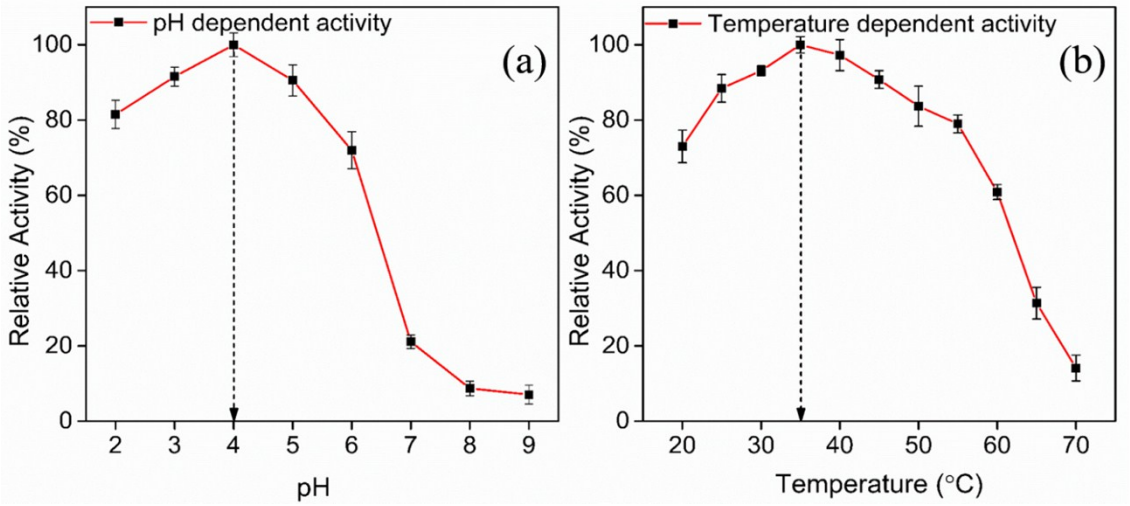

Figure S2. Peroxidase activity of 5SCP-800 recorded at different pH conditions at room temperature (a) and different temperature at a fixed pH 4.0 (b).

pH and temperature dependent peroxidase activity

Detection of hydroxyl radicals

Typically, a 5 mL reaction volume containing aqueous solution of TA (0.5 mM) prepared in NaOH solution (2 mM) and, 0.2 M H_2O_2 and 10 µg/mL of SCP nanorods. Emission spectra was recorded with an excitation wavelength of 315 nm after an incubation period of 1 hour under dark condition. When TA (non-fluorescent) reacting with hydroxyl radical, forms

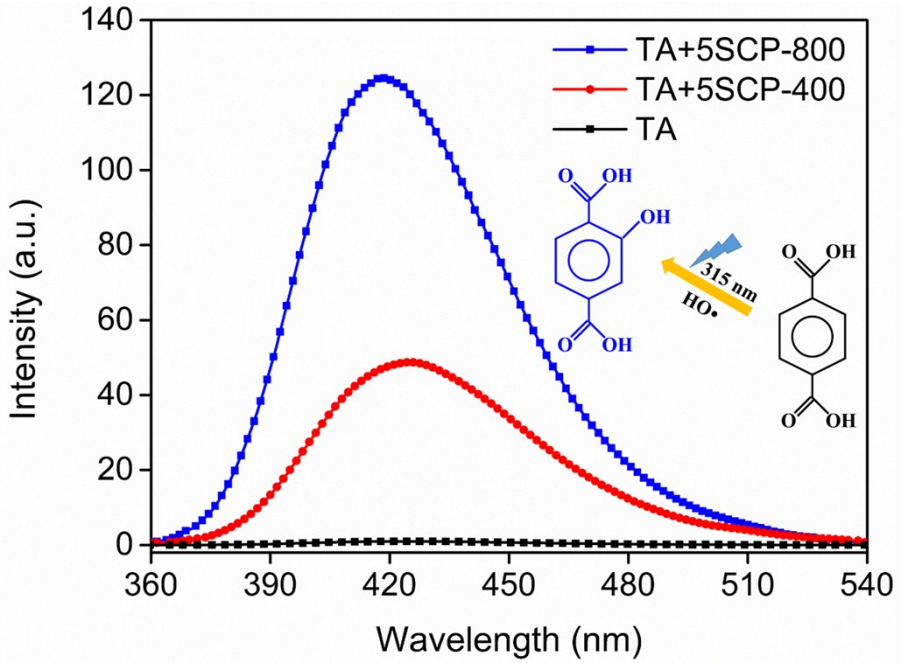

Figure S3. Fluorescent emission of terephthalic acid in the presence of hydroxyl radicals (excited at a wavelength 315 nm) by monitoring the emission at 425 nm

2-hydroxyterephthalic acid which gives fluorescence around 425 nm. The peak observed at 422 nm (Fig. S3) in our case indicates the formation of hydroxyl radicals when H_2O_2 interact with SCP nanorods. The size (Table 1) and surface area of the 5SCP-400 (48.29 m^2g^{-1}) and 5SCP-800 (43.31 m^2g^{-1}) have no effect on the peroxidase activity due to its negligible difference. Although the clear mechanism of peroxidase activity is yet to be understood with respect to the structural aspects, the monoclinic SCP is efficient in the generation of hydroxyl radicals. This observation is in agreement with the superior peroxidase activity of monoclinic SCP nanorods observed in UV-Vis analysis. Presence of mixed oxidation state of Ce^{3+}/Ce^{4+}

confirmed by XPS analysis, the formation of Ce^{4+} sites under oxidizing condition further enhance redox transformation between $Ce^{3+} \leftrightarrow Ce^{4+}$ sites at the surface of SCP nanorods.

Raman spectra of SCP treated with H_2O_2

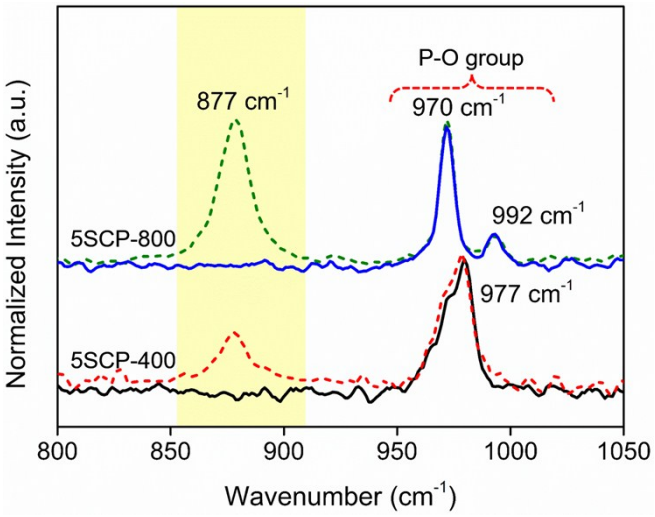

Figure S4. Raman spectra of as-prepared hexagonal (5SCP-400) and monoclinic (5SCP-800) nanorods (solid line) and treated with hydrogen peroxide (dashed line)

Figure S4 shows the Raman spectra of the as-prepared and hydrogen peroxide treated (100 mM, incubated for 2 hours and dried overnight at 50º C) SCP nanorods. Room temperature Raman spectra obtained using 785 nm laser source clearly distinguished the hexagonal (977 cm^{-1}) and monoclinic structure (970 cm^{-1} and 992 cm^{-1}) in the hydrogen peroxide treated and untreated SCP nanorods. A sharp peak at 877 cm^{-1} observed for H_2O_2 treated SCP was absent on the as-prepared samples. The band at 877 cm^{-1} was intense in monoclinic SCP compared to hexagonal structure. It can be attributed to the surface adsorbed H_2O_2/surface-peroxo species formed when H_2O_2 interacts with cerium phosphate.

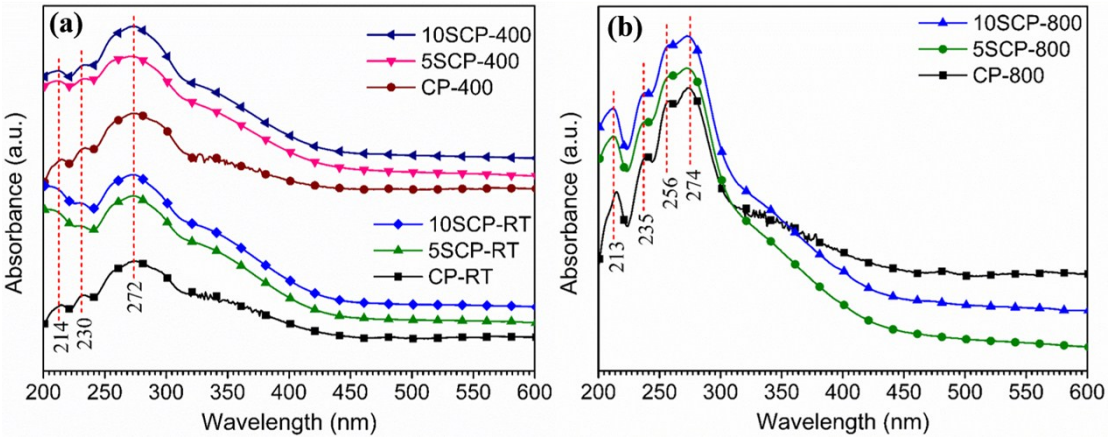

Figure S5. UV-Vis absorption spectra of hexagonal (a) and monoclinic (b) $CePO_4$

UV-Visible Spectra

The UV-Vis absorbance spectra of the $CePO_4$ nanorods are shown in Figure S3 (a and b). The spectra shown in Figure S3a of the as-prepared and 400 °C annealed hexagonal $CePO_4$ show three bands centered around 214, 230 and 272 nm while the samples annealed at 800 °C displayed an additional peak at 256 nm. Generally, the Ce^{3+} ions exhibit 4f-5d transition which lies in the ultra-violet region. The additional peaks observed for the monoclinic structure can be attributed to the crystal field splitting of $5d^1$ levels of Ce^{3+} ions[3].

Oxidation-reduction of SCP nanorods using Optical absorption spectra

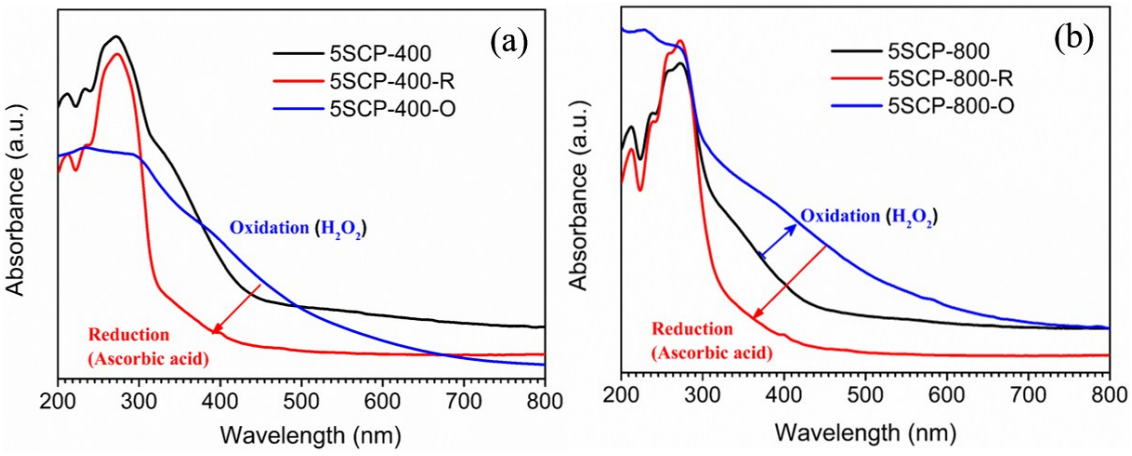

Figure S6. Oxidation and reduction treatment of hexagonal 5SCP-400 (a) and monoclinic 5SCP-800 (b) using H_2O_2 and ascorbic acid, respectively.

The broad absorption in the visible range can be attributed to the presence of Ce^{4+} ions states irrespective of the crystal structure. The broad peak in the visible region can be attributed to the strong electron-phonon coupling in their d-electron excited states[3]. To understand this difference in catalytic activity, the selected samples were subjected to oxidation and reduction treatments using H_2O_2 and ascorbic acid, respectively, and the corresponding absorption spectra is shown in Figure S4. When the samples are oxidized, the absorption features of monoclinic structure extend well into the visible region compared to hexagonal sample as shown in Figure S4. Higher absorption in the visible region by monoclinic SCP is a direct evidence for the presence of more Ce^{4+} sites than hexagonal samples. Further when the oxidized samples were reduced by ascorbic acid, the absorption band edge falls within 200-300 nm region of the spectra. As discussed earlier, the absorption bands observed below 350 nm corresponds to Ce^{3+} species of cerium phosphate. The redox cycling between $Ce^{3+} \leftrightarrow Ce^{4+}$ in ceria-based materials responsible for redox luminescent switching properties might hold true for the enhanced peroxidase like mimetic activity in monoclinic cerium phosphate nanostructures[4-6].

Selectivity and Repeatability of H_2O_2 sensing

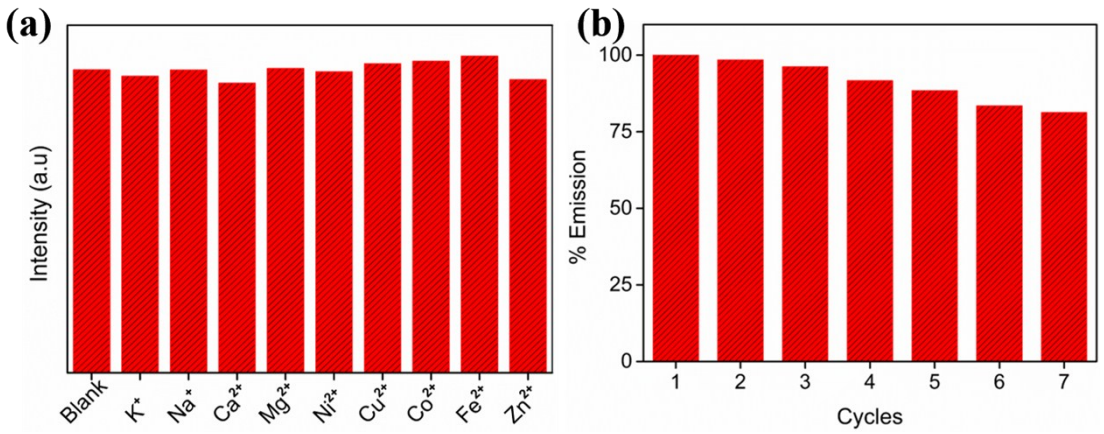

Figure S7. Selectivity competition for the sensing of hydrogen peroxide (150 µM) using 5SCP-800 (10 µM) in the presence of various interfering ions of 50 µM concentration (a) and Stability of fluorimetric H_2O_2 sensor using 5CP-800 nanorods (b)

EDAX spectrum of Sm^{3+} doped Cerium phosphate (5SCP)

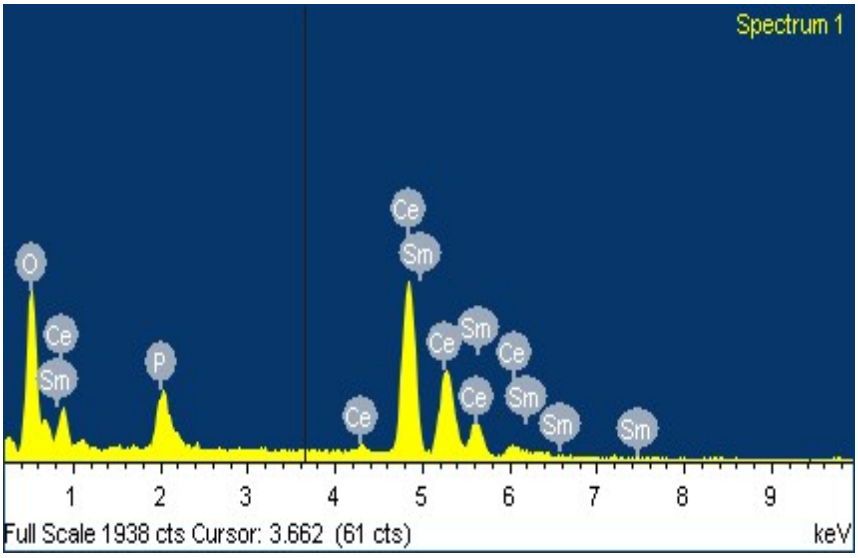

Figure S8. A representative EDAX spectrum of Sm^{3+} doped cerium phosphate nanorods (5SCP)

Table S1. Comparison chart for H_2O_2 peroxide sensing by different methods

Material	Method	Linearity	LOD	Reference
CeO_2/TiO_2	Calorimetric	5 to 100 µM	3.2 µM	[7]
$HAQB/GO_x$	Fluorimetric	8 to 420 µM	11 µM	[8]
CeO_2 – DNA	Fluorimetric	1 to 100 µM	0.64 µM	[9]
CeO_2-APTS	Calorimetric	2.5 to 100 mM	0.05 mM	[10]
$CePO_4$:Tb,Gd	Calorimetric	1×10^{-5} to 5×10^{-4} M	0.005 mM	[11]
$CePO^4$: Sm^{3+}	Fluorimetric	1 to 150 µM	3.1 µM	This work

References

(1) Patra, C. R.; Alexandra, G.; Patra, S.; Jacob, D. S.; Gedanken, A.; Landau, A.; Gofer, Y. Microwave Approach for the Synthesis of Rhabdophane-Type Lanthanide Orthophosphate (Ln = La, Ce, Nd, Sm, Eu, Gd and Tb) Nanorods under Solvothermal Conditions. *New J. Chem.* **2005**, *29*, 733–739.

(2) Verma, S.; Bamzai, K. K. Preparation of Cerium Orthophosphate Nanosphere by Coprecipitation Route and Its Structural, Thermal, Optical, and Electrical Characterization. *J. Nanoparticles* **2014**, *2014*, 1–12.

(3) Tang, C.; Bando, Y.; Golberg, D.; Ma, R. Cerium Phosphate Nanotubes: Synthesis, Valence State, and Optical Properties. *Angew. Chemie.* **2005**, 117, 582-585.

(4) Kitsuda, M.; Fujihara, S. Quantitative Luminescence Switching in $CePO_4$:Tb by Redox Reactions. *J. Phys. Chem. C.* **2011**, *115*, 8808–8815.

(5) Jampaiah, D.; Srinivasa Reddy, T.; Kandjani, A. E.; Selvakannan, P. R.; Sabri, Y. M.; Coyle, V. E.; Shukla, R.; Bhargava, S. K. Fe-Doped CeO_2 Nanorods for Enhanced Peroxidase-like Activity and Their Application towards Glucose Detection. *J. Mater. Chem. B* **2016**, *4*, 3874–3885.

(6) Liu, Y.; Zhu, G.; Yang, J.; Yuan, A.; Shen, X. Peroxidase-Like Catalytic Activity of Ag_3PO_4 Nanocrystals Prepared by a Colloidal Route. *PLoS One.* **2014**, *9*, e109158:1-7.

(7) Zhao, H.; Dong, D.; Jiang, P.; Wang, G.; Zhang, J.; Hihgly Dispersed CeO_2 on TiO_2 Nanotube: A synergistic Nanocomposite with superior Peroxidase-Like Activity. *ACS Appl. Mater. Interfaces.* **2015,** *7***,** 6451-6461.

(8) Wannajuk, K.; Jamkatoke, K.; Tuntulani, T.; Tomapatanaget, B.; Highly Specific-Glucose Fluorescence Sensing Based on Boronic Anthraquinone Derivatives via the GOx enzymatic reaction. *Tetrahedron.* **2012,** *68*, 8899-8904.

(9) Gao, W.; Wei, X.; Wang, X.; Cui, G.; Liu, Z.; Tang, B.; A competitive coordination-based CeO2 nanowire-DNA Nano sensor: fast and selective detection of hydrogen peroxide in living cells and in vivo. *Chem.Comm.* **2016,** *52*, 3643-3646.

(10) Ornatska, M.; Sharpe, E.; Andreescu, D.; Andreescu, S.; Paper Bioassay Based on Ceria Nanoparticles as Calorimetric Probes. *Anal. Chem.* **2011,** *83*, 4273-4280.

(11) Wang, W.; Jiang, X.; Chen, K.; $CePO_4$: Tb, Gd hollow nanospheres as peroxidase mimic and magnetic-fluorescent imaging agent. *Chem.Comm.* **2012,** *48*, 6839-6841.